Transactions, SMiRT-26
Berlin/Potsdam, Germany, July 10-15, 2022
Division III

VALIDATION OF NONLINEAR SOIL-STRUCTURE INTERACTION IN MASTODON

Samyog Shrestha[1], Efe G. Kurt[2], Kyungtae Kim[3], Arun Prakash[4], and Ayhan Irfanoglu[5]

[1]PhD Student, Purdue University, West Lafayette, IN, USA (shresth3@purdue.edu)
[2]Research Scientist, Idaho National Lab, Idaho Falls, ID, USA
[3]Transportation Engineer, California Department of Transportation, CA, USA
[4]Associate Professor, Lyles School of Civil Engineering, Purdue University, West Lafayette, IN, USA
[5]Professor, Lyles School of Civil Engineering, Purdue University, West Lafayette, IN, USA

ABSTRACT

Validation of nonlinear soil-structure interaction analysis in MASTODON (open-source finite element code) is performed using experimental data from a shake table test. Discrepancy metric proposed by Sprague and Geers is used to evaluate agreement between computed and measured response histories at selected locations in the model. The computed acceleration, velocity, displacement and racking deformation are found to have good to fair agreement with measured response.

INTRODUCTION

The term SSI appeared in literature in 1960's when nuclear power plants were designed in seismic regions such as California. In early 1970's, rigorous solutions were developed to solve problems of dynamically loaded circular footings on linear elastic soil. It spurred further research on methods to solve SSI problems. Today, such methods can be broadly categorized into direct approach and impedance (sub-structure) approach [Kramer (1996)].

In impedance approach, the soil-foundation interaction is represented by spring/dashpot system and free-field soil motion is converted into foundation input motion to account for presence of structure. Solution to the SSI problem is obtained by applying foundation input motion to the combined structure – spring/dashpot system. This technique is based on linear superposition and cannot capture nonlinear behaviour directly. In direct approach, the entire soil-foundation-structure system is modelled and analysed together in time domain with appropriate boundary conditions. This approach can capture material nonlinearity as well as sliding and separation at soil-structure interface. But, it is computationally expensive due to requirement of modelling large soil domain.

With development of numerical methods and improvement in computational ability, nonlinear SSI methods are being used for more realistic simulations. However, all aspects of the real-world condition cannot be captured fully due to intrinsic numerical complexity (e.g. restricting frequency captured by numerical model, tolerating boundary artifacts), intrinsic material complexity (e.g. spatial inhomogeneities in soil) and intrinsic seismic complexity (e.g. not knowing the actual ground motion) [Kausel (2007)]. When such complexities are not critical, numerical results from nonlinear SSI analysis should provide a good approximation of the observed behaviour.

To evaluate reliability of numerical codes, numerical results are validated against analytical solution, experimental result or other valid numerical solutions [Jauregui and Silva (2011)]. Often visual

comparison is not sufficient when large data sets are involved. SSI analyses produce solutions in the form of response histories. In such cases, point-to-point comparison between reference and numerical solution at each time instant [e.g. Sprague and Geers (2004)] provides better evaluation [Schwer (2007)]. Generally validation methods provide a single value that serves as a measure of agreement or discrepancy between numerical and reference solutions.

Validation of nonlinear SSI analysis tools is limited in literature due to lack of large-scale experiments and complex nature of SSI problems due to which analytical solutions are not available. The current study presents validation of an open-source 3-dimensional finite element code called MASTODON [Coleman et al. (2017)] using experimental data from shake table test of a steel tunnel embedded in soil.

BRIEF DESCRIPTION OF EXPERIMENT

The first among a series of 1/9 scale tests performed at University of California, San Diego [Kim and Elgamal (2017)] is considered which consists of the tunnel with 0.6 m (2 ft) deep overburden soil as shown in *Figure 1*. A laminar box 6.7 m (22 ft) long, 2.9 m (9.6 ft) wide and 4.4 m (14.5 ft) high was used in the test. The laminar box was filled with sand and a tunnel was placed between 2.8 m (9.3 ft) and 3.8 m (12.6 ft) from the base as shown in *Figure 1*. The tunnel was made of hollow steel sections at its base and roof, steel plate walls (~20 mm or 0.75 in thick) and wooden roof. Cross-section of the tunnel was about 1.8 m (6 ft) x 1 m (3.25 ft) and it extended the entire width of the soil (2.8 m or 9.3 ft). The laminar box was mounted on top of a shake table which was excited laterally (in one direction only) by a scaled version of the 1994 Northridge earthquake recorded at Fire Station 108, 12520 Mulholland Dr., USC station 5314 (Component 35). The resulting motion of the shake table presented in *Figure 2*, is used as the input motion for numerical simulation.

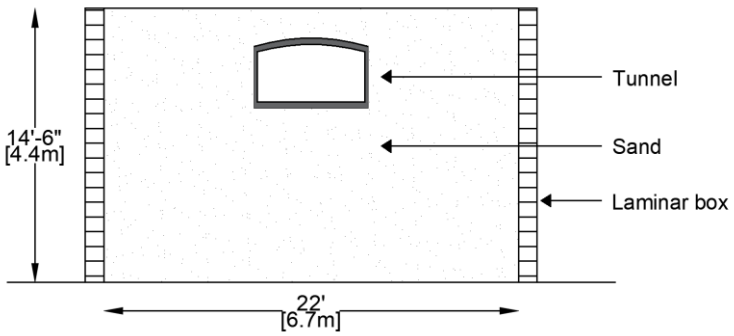

Figure 1: Typical section of tunnel-soil model

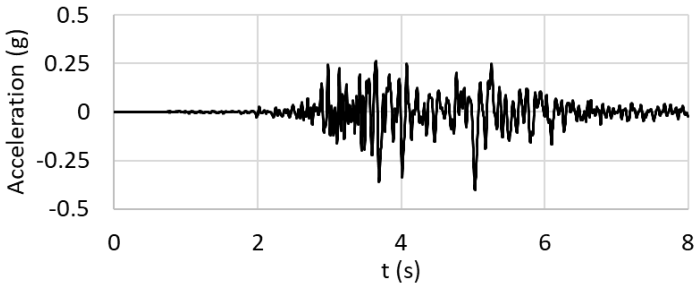

Figure 2: Input motion

NUMERICAL MODELLING

Figure 3 presents tunnel-soil model created for analysis in MASTODON. The hollow structural steel sections in the physical model are represented by uniform plates (~ 0.15 m or 6 in thick) in the numerical model with density adjusted to account for their actual weight. Lateral deformation of the tunnel is caused by out-of-plane stiffness of the wall. Base plate, roof plate and wooden roof are rigid compared to the wall. Material properties used in analysis are summarized in *Table 1*. Since the tunnel remained in linear elastic range during the shake table test [Kim and Elgamal (2017)], it is modelled by elastic material. Using material properties tabulated in *Table 1*, the computed lateral stiffness of the tunnel is approximately equal to the reported value of 21.5 kN/mm (123 kip/in). Both soil and tunnel are modelled using 20-noded brick elements (C3D20).

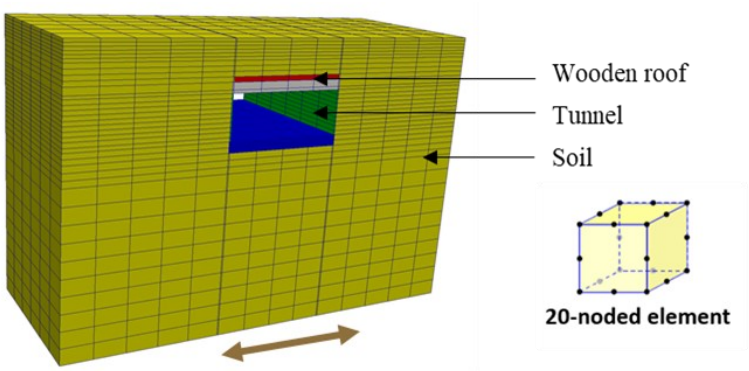

Figure 3: Numerical model in MASTODON

Table 1: Material properties of tunnel

SN	Property	Base plate	Roof plate	Wooden roof	Wall
1	Unit weight kN/m^3 (pcf)	29.8 (190)	6.1 (39)	0.9 (6)	77 (490)
2	Elastic modulus GPa (ksi)	Rigid compared to wall			200 (29000)
3	Poisson's ratio	0.3	0.3	0.3	0.3

Shear wave velocity profile measured during the series of experiments showed variability between shaking events particularly for soil below the level of tunnel base. Average shear modulus for soil above the tunnel base was around 18.1 MPa (2625 psi). Reference shear modulus for soil below the tunnel base is taken as 55.4 MPa (8030 psi) such that the fundamental frequency of the model matches with reported value. Soil properties representative of the particular test considered in this study are tabulated in Table *2*.

Shear wave velocity of soil also exhibited pressure dependency. To model pressure dependency, reference confining pressure is taken corresponding to the mid-height of the model which works out to be 29.6 KPa (4.3 psi). Shear modulus at any depth is obtained as given in Eq. 1.

$$G(z) = G_{ref}\left[\frac{p(z)}{p_{ref}}\right]^{0.5} \quad (1)$$

where, G_{ref} is reference shear modulus, p_{ref} is reference confining pressure, $G(z)$ and $p(z)$ are respectively shear modulus and confining pressure at depth z. The resulting shear wave velocity profile is shown in Figure 4. As shown in the figure, 28 soil layers are considered. Soil within the extent of tunnel wall is considered as a single layer.

Table 2: Soil properties

Properties	**Values**	
	Below tunnel base	**Above tunnel base**
Reference shear modulus, MPa (psi)	55.4 (8030)	18.1 (2625)
Reference confining pressure, KPa (psi)	29.6 (4.3)	29.6 (4.3)
Poisson's ratio	0.4	0.4
Unit weight, kN/m³ (pcf)	18.9 (120)	18.9 (120)
Friction angle (degrees)	52	52
Cohesion, KPa (psi)	13.8 (2)	13.8 (2)

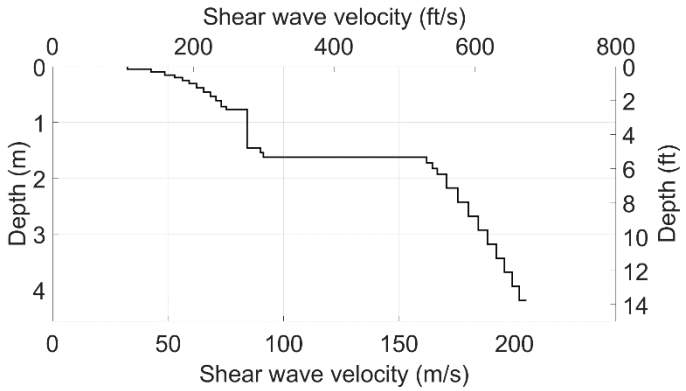

Figure 4: Shear wave velocity profile of soil

Nonlinear soil properties are modelled using backbone curve [Groholski et al. (2016)] shown in Eq. 2.

$$\tau = \frac{\tau_{max}}{2}\left[\frac{1}{\theta_\tau}\left(1+\frac{\gamma}{\gamma_r}-\sqrt{\left(1+\frac{\gamma}{\gamma_r}\right)^2-4\theta_\tau\frac{\gamma}{\gamma_r}}\right)\right] \tag{2}$$

where, τ is shear stress, γ is shear strain, θ_τ is a curve fitting parameter, γ_r is the ratio of shear strength and low-strain shear modulus, and τ_{max} is shear strength obtained from Mohr-Columb relation presented in Eq. 3.

$$\tau_{max} = c + p\,sin\,\phi \tag{3}$$

where, c and ϕ are cohesion and friction angle as provided in Table *2*, and p is confining pressure which is dependent on mid-depth of soil layers.

The curve-fitting parameter θ_τ is obtained using reference modulus reduction curve proposed by Darendeli [Darendeli (2001)] for Southern California sand. The reference modulus reduction curve is obtained for mid-height of the model which has a confining pressure of 29.6 KPa (4.3 psi) and assuming that the plasticity index of sand is zero. Figure 5 presents normalized modulus reduction and backbone curves for the soil layer at mid-height of the model. Reference values obtained from Darendeli are plotted up to a strain of 0.1% and shear strength is plotted at 10% strain. A value of θ_τ = -7 is found to provide a good fit, which is used in Eq. 2 to define backbone curve for soil layers. For the top-most soil layer having thickness of around 5 cm (~ 2 in), the value of θ_τ is taken as -4.

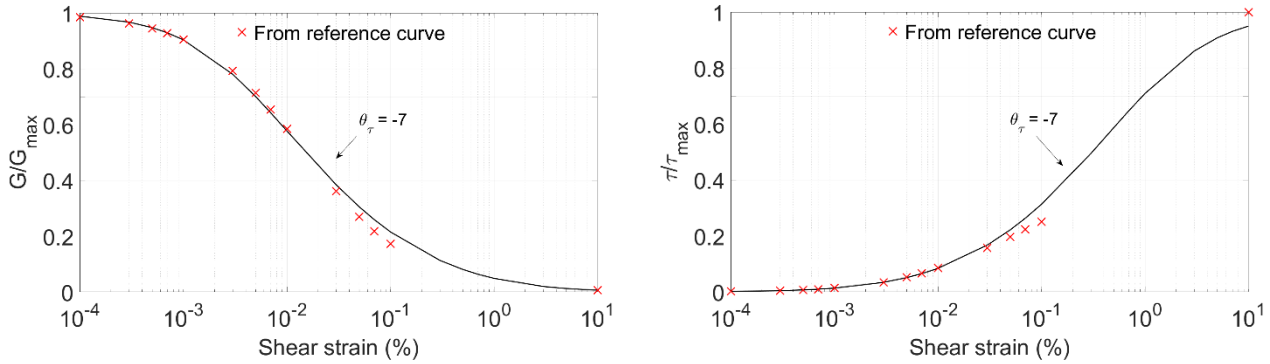

(a) Modulus reduction curve (b) Backbone curve

Figure 5: Nonlinear soil properties

Input acceleration is prescribed uniformly at the base of the tunnel-soil model. It is applied parallel to the length of the model (direction indicated in *Figure 3)*. The base of the numerical model is fixed in other directions. Vertical faces of the tunnel-soil numerical model at the outer boundary are constrained to move together at each elevation, thus simulating pure shear behaviour. The tunnel and soil are tied together at the interface. Analysis is done using Hilber-Hughes-Taylor integration scheme (β = 0.4225, γ = 0.8, α = -0.3) with a time-step of 0.00417s.

SOIL MATERIAL MODEL

A piecewise linearized nonlinear hysteretic soil model available in MASTODON is used. In one dimensional shear stress space, the model is represented by nested spring and slider components of different. The model behaviour is obtained by superimposing the stress-strain response of those nested components. Three dimensional generalization uses Von Mises yield criterion and an associative flow rule. The soil model utilizes Masing rule for hysteretic reloading/unloading formulation. Therefore, Masing type of hysteretic damping model is implemented. Additional damping is applied to simulate soil behaviour at small strain. In this study, stiffness dependent parameter, ζ = 0.000603 and mass dependent parameter, η = 3.98 are used, which simulates Rayleigh damping of 5% nearly constant over the first few modes of the model (fundamental frequency, f_0 ~ 9 Hz).

CALIBRATION OF SOIL BACKBONE CURVE

Structural response is affected by uncertainty in material properties. A sensitivity study based on nonlinear soil-structure interaction analysis showed that the acceleration and roof drift in a generic embedded structure varied by 20% to 25% when realistic range of uncertain material properties were considered [Shrestha et al. (2022)]. Soil properties were found to be more sensitive to structural response with increasing shear strain in soil layers.

Material properties used in this study are, in general, obtained either from direct measurement or evaluated based on reported secondary information. But, nonlinear soil properties are based on assumed modulus reduction curves which can cause discrepancy between computed and measured response. To capture the sensitivity of numerical results to nonlinear soil properties, two analyses are conducted using backbone curves defined by the following parameters:

- Using parameter θ_τ = -4 for the top-most soil layer, and θ_τ = -7 for other layers.
- Using θ_τ = -1 for soil within the extent of the tunnel wall, θ_τ = -4 for the top-most soil layer, and θ_τ = -7 for other layers.

The first analysis is based on Darendeli's reference modulus reduction curve. The second analysis is based on calibrated nonlinear soil properties. Discrepancy between measured and computed response is evaluated for both analyses and compared based on discrepancy metric proposed by Sprague and Geers.

VALIDATION METHOD

In this study, discrepancy between measured and computed response, denoted by *m(t)* and *c(t)* respectively, is quantified using discrepancy metrics developed by Sprague and Geers. They proposed Eq. 4 to account for magnitude difference and Eq. 5 to account for phase difference.

$$M_{SG} = \sqrt{\frac{e_{cc}}{e_{mm}}} - 1 \tag{4}$$

$$P = \frac{1}{\pi} cos^{-1}\left(e_{mc} / \sqrt{e_{cc}\, e_{mm}} \right) \tag{5}$$

where,

$$e_{cc} = \int c(t)\, c(t)\, dt$$

$$e_{mm} = \int m(t)\, m(t)\, dt$$

$$e_{mc} = \int m(t)\, c(t)\, dt$$

Each index considers the entire response histories of computed and measured solution and provides a single value using integrals. The two indices are insensitive to one another and are combined together as shown in Eq. 6. Discrepancy below 20% is considered as good, between 20% and 30% is considered as fair, and above 30% is considered as poor agreement [Sprague and Geers (2004)].

$$C_{SG} = \sqrt{M_{SG}^2 + P^2} \tag{6}$$

OBSERVATIONS

The computed response is compared with measured response from accelerometers located at three soil depths 0 m (0 ft), 1.6 m (5.3 ft) and 3.1 m (10.3 ft) from the soil surface. Analysis results are presented using calibrated nonlinear soil properties. Comparison of acceleration time-series is presented in *Figure 6*. Peak acceleration of around 0.6 g is computed at surface level which agrees with the test result. Computed acceleration response showed better agreement with measured response for soil layers closer to the shake table.

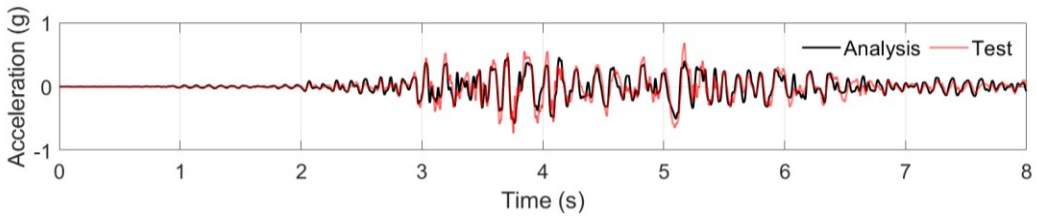

(a) At depth 0 m (0 ft)

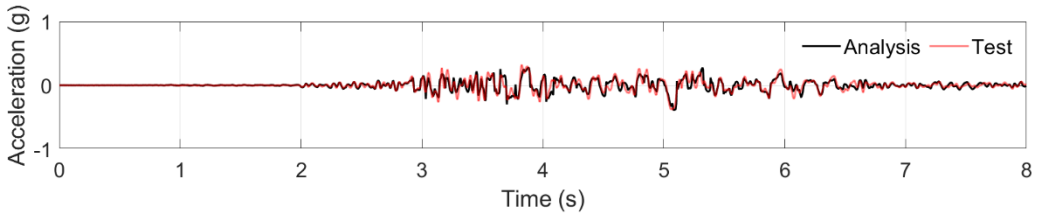

(b) At depth 1.6 m (5.3 ft)

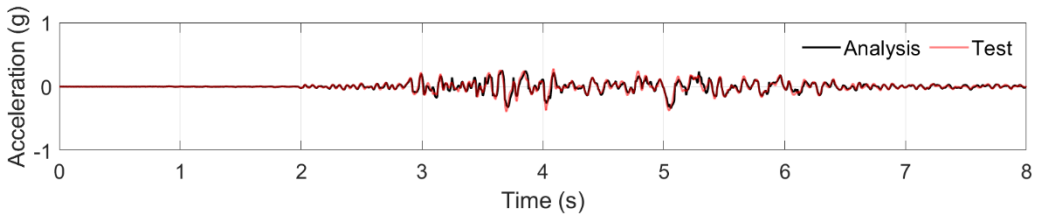

(c) At depth 3.1 m (10.3 ft)

Figure 6: Comparison of acceleration response in soil

Differences between analysis and test acceleration response can be comprehended from their spectral acceleration response. 5% damped acceleration response spectra are presented in *Figure 7* for three soil depths. Measured and computed top-of-soil response are identical up to a frequency of 2 Hz but gradually deviates in the frequency range of 2 Hz to 9 Hz. Beyond 9 Hz, measured and computed spectra are similar but differences exist above 30 Hz. At soil depth of 1.6 m (5.3 ft), measured and computed spectral acceleration differ by around 10% on average over the frequency range 0.1 to 100 Hz. Acceleration response at soil depth of 3.1 m (10.3 ft) is captured almost identically across the frequency range.

A comparison of velocity time-series is presented in *Figure 8* for three soil depths. Velocity response is based on integration of measured and computed acceleration. Observations are similar to that observed in the comparison of acceleration response but discrepancies in the high frequency range are eliminated as a result of integration. Discrepancy between computed and measured response decreases with

soil depth. The analysis almost replicates measured velocity at depths of 1.6 m (5.3 ft) and 3.1 m (10.3 ft) from the soil surface.

Figure 9 shows lateral soil displacement at different depths relative to the base of the tunnel-soil assembly. Computed displacements are compared to measurements on the soil container. Displacement at different depths was obtained from displacement sensors (string potentiometers) attached centrally to one of the short edges of the laminar box. The peak displacement is around 10 cm (~ 4 in) at the soil surface. At all three depths considered, discrepancy between measured and computed displacements are larger compared to velocity and acceleration response.

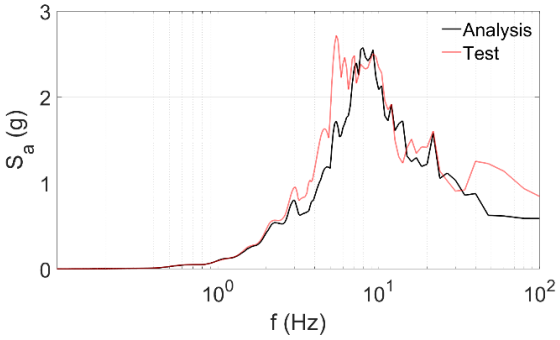

(a) At depth 0 m (0 ft)

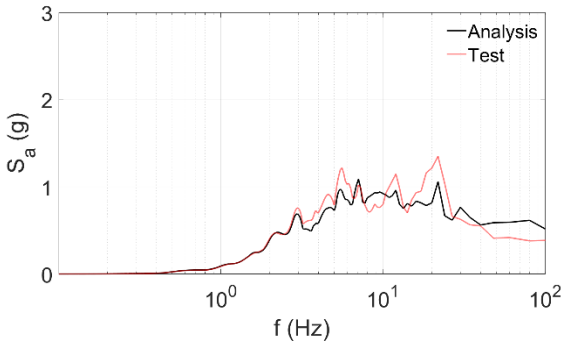

(b) At depth 1.6 m (5.3 ft)

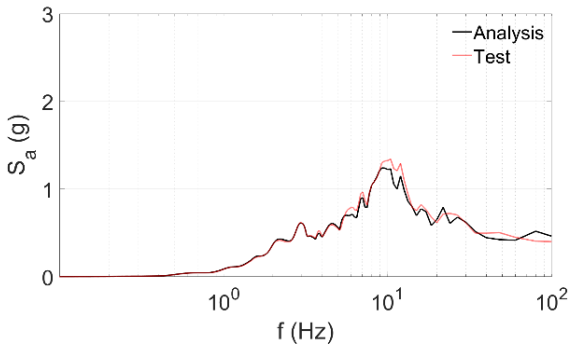

(c) At depth 3.1 m (10.3 ft)

Figure 7: Comparison of spectral acceleration in soil

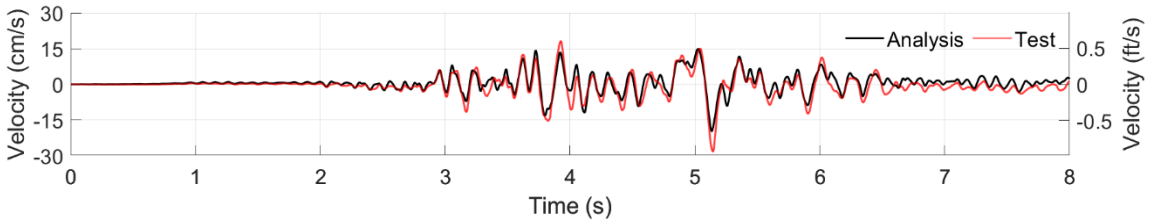

(a) At depth 0 m (0 ft)

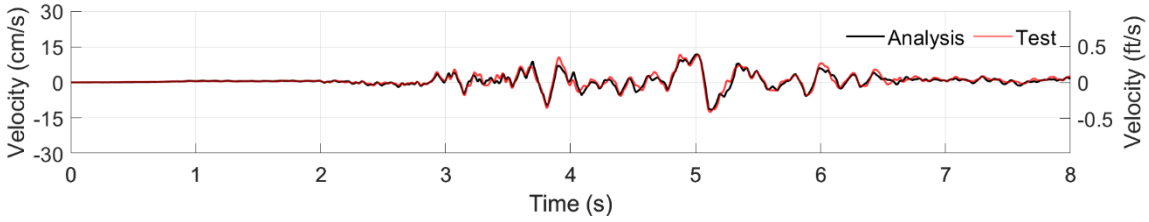

(b) At depth 1.6 m (5.3 ft)

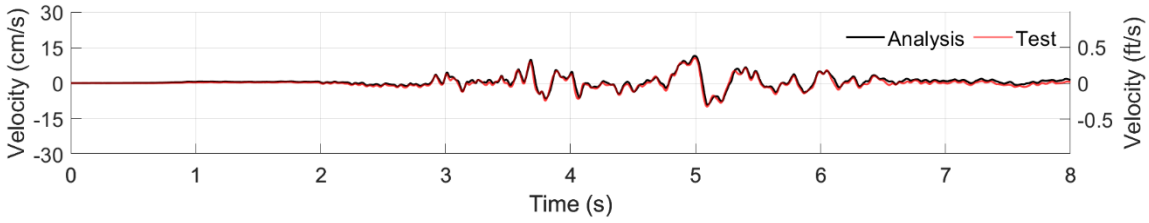

(c) At depth 3.1 m (10.3 ft)

Figure 8: Comparison of velocity response in soil

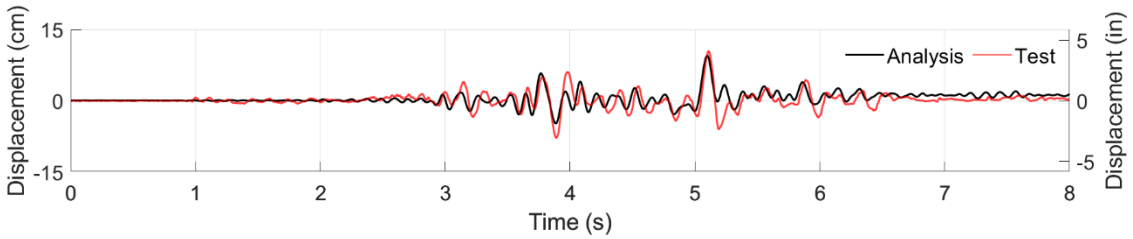

(a) At depth 0 m (0 ft)

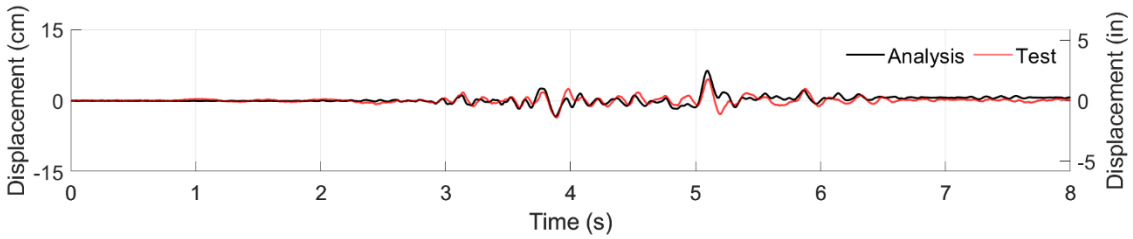

(b) At depth 1.6 m (5.3 ft)

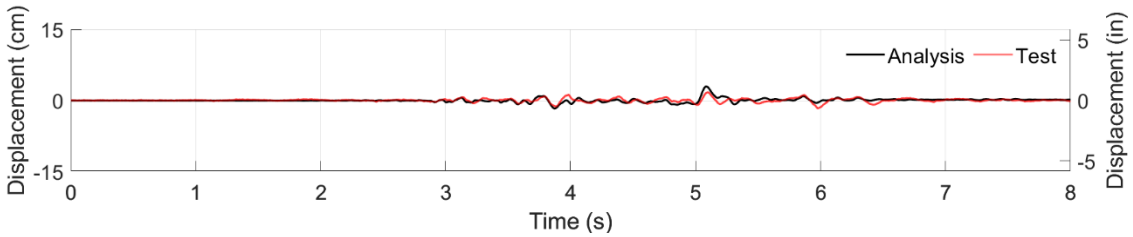

(c) At depth 3.1 m (10.3 ft)

Figure 9: Comparison of relative displacement in soil

The racking response of tunnel wall is shown in *Figure 10*. In MASTODON, it is calculated by subtracting displacement due to rigid body rotation of tunnel, to the relative displacement between the top and bottom of the tunnel wall in the direction of shaking. From the shake table test, it was measured from displacement sensors (linear potentiometers) placed inside the tunnel which measures only flexural displacements. There is resemblance in frequency content of displacement response in the tunnel but differences in magnitude exist throughout the shaking duration. Peak tunnel racking response is estimated to be about 0.2 cm (0.08 in) which agrees with that measured during the experiment.

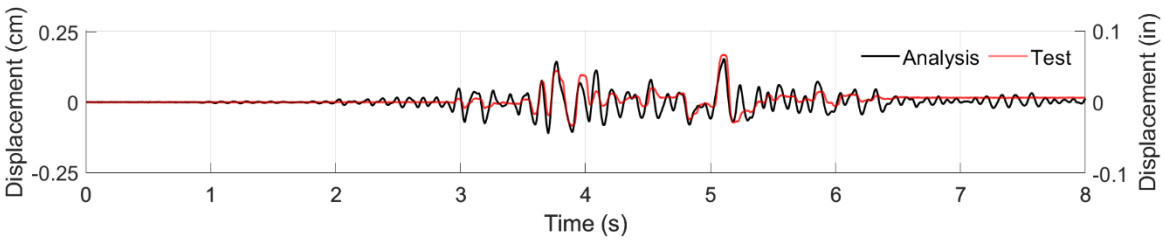

Figure 10: Tunnel racking response

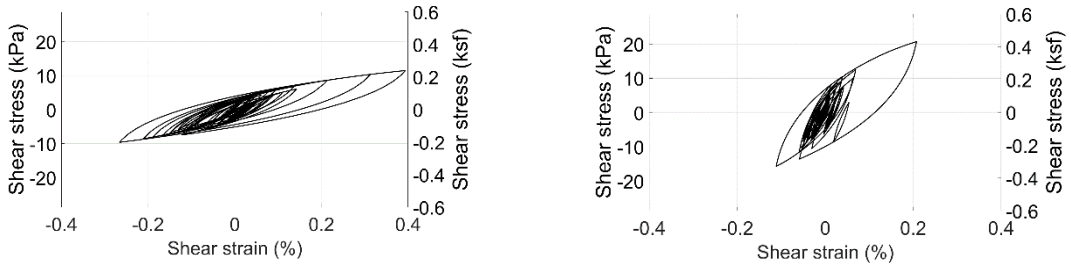

(a) At depth 1.6 m (5.3 ft) (b) At depth 3.1 m (10.3 ft)

Figure 11: Computed stress-strain in soil

Soil layers within the extent of tunnel developed shear strain up to 0.4% as indicated in Figure 11. Referring to Figure 5, shear modulus at a strain of 0.4% is less than 20% of low-strain shear modulus (G_{max}). This makes analysis results sensitive to nonlinear soil properties. To evaluate sensitivity of nonlinear soil properties, two analyses were conducted by varying nonlinear parameters of soil. Discrepancies between computed and measured response were evaluated for each analysis. A summary of discrepancy between computed and measured response is presented in *Figure 12*.

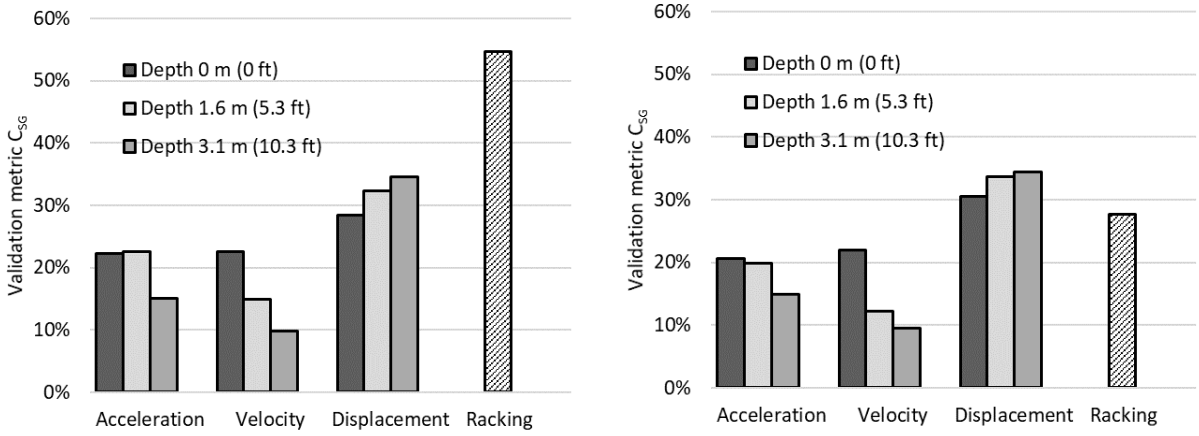

(a) Using reference backbone curves (b) Using calibrated backbone curves

Figure 12: Discrepancy metric between computed and measured response

In the figure, combined validation metric (C_{SG}) is shown for various responses compared in this study using reference and calibrated backbone curves for soil. Soil response (acceleration, velocity, and relative displacement) are, in general, within 10 to 30% which indicates good to fair agreement between computed and measured response. Tunnel racking response has a poor agreement with experimental data (discrepancy exceeding 50%) when reference backbone curves are used. Although lateral stiffness of tunnel without the surrounding soil was identical for the model and the experiment, there was no information regarding lateral stiffness of tunnel when surrounded by soil. It was observed that the tunnel used in the experiment behaved stiffer during the shake table test compared to the numerical model. Backbone curve for soil at the tunnel level is modified to model a stiffer response of the tunnel-soil assembly.When calibrated backbone curves are used for soil layer at the tunnel level, discrepancy metric for tunnel racking deformation reduced to below 30% which indicates fair agreement between measured and computed response.

SSI analysis described in this study captured overall physics of the shake table test. Nevertheless, it must be noted that uncertainties exist in terms of numerical modelling (assumptions made for soil-structure contact and behaviour of laminar box) and soil properties (assumption made for nonlinear properties of soil) which cause errors in numerical analysis.

CONCLUSION

From visual inspection of analysis results, it can be inferred that MASTODON can solve nonlinear soil-structure interaction problems and produce results comparable to the test results. Good to fair agreement was found in terms of soil response and tunnel racking deformation as indicated by the discrepancy metric used in this study. Sensitivity of nonlinear soil properties on computed response was also evaluated which was found to be significant for tunnel racking deformation.

REFERENCES

Coleman, J., Slaughter, A., Veeraraghavan, S., Bolisetti, C., Numanoglu, O. A., Spears, R., Hoffman, W., and Kurt E. G. (2017). "MASTODON theory manual (No. INL/EXT-17-41930)," Idaho National Lab (INL), Idaho Falls, ID, United States.

Darendeli, M. B. (2001). "Development of a new family of normalized modulus reduction and material damping curves," The university of Texas at Austin.

Groholski, D. R., Hashash, Y. M., Kim, B., Musgrove, M., Harmon, J., & Stewart, J. P. (2016). "Simplified model for small-strain nonlinearity and strength in 1D seismic site response analysis," *Journal of Geotechnical and Geoenvironmental Engineering*, *142*(9), 04016042.

Kim, K., and Elgamal, A. (2017). "Cut-and-Cover Tunnel Shake Table Test Program," University of California San Diego, La Jolla.

Jauregui, R., and Silva, F. (2011). "Numerical validation methods," *Numerical analysis—theory and application*, 155-174.

Kausel, E. (2007). "Comments on soil-structure interaction," *The 4th UJNR Workshop on Soil-Structure Interaction*, *Tsukuba Japan* (Vol. 1).

Kramer, S. L. (1996). "Geotechnical earthquake engineering," Pearson.

Schwer, L. E. (2007). "Validation metrics for response histories: perspectives and case studies," *Engineering with Computers*, *23*(4), 295-309.

Shrestha S., Kurt E., Abdelaleim O., Prakash A., and Irfanoglu A. (Forthcoming), "Sensitivity study on parameters influencing soil-structure interaction of embedded structure" In *12th National Conference on Earthquake Engineering, 2022,* Earthquake Engineering Research Institute.

Sprague, M. A., and Geers, T. L. (2004). "A spectral-element method for modelling cavitation in transient fluid–structure interaction," *International Journal for Numerical Methods in Engineering*, *60*(15), 2467-2499.